RSC Advances

This is an *Accepted Manuscript*, which has been through the Royal Society of Chemistry peer review process and has been accepted for publication.

Accepted Manuscripts are published online shortly after acceptance, before technical editing, formatting and proof reading. Using this free service, authors can make their results available to the community, in citable form, before we publish the edited article. This *Accepted Manuscript* will be replaced by the edited, formatted and paginated article as soon as this is available.

You can find more information about *Accepted Manuscripts* in the Information for Authors.

Please note that technical editing may introduce minor changes to the text and/or graphics, which may alter content. The journal's standard Terms & Conditions and the Ethical guidelines still apply. In no event shall the Royal Society of Chemistry be held responsible for any errors or omissions in this *Accepted Manuscript* or any consequences arising from the use of any information it contains.

ROYAL SOCIETY OF CHEMISTRY

www.rsc.org/advances

Goethite Nanorods as Cheap and Effective Filler for Siloxane Nanocomposite Elastomers

M. Iacob, G. Stiubianu, C. Tugui, L. Ursu, M. Ignat, C. Turta and M. Cazacu

Composites based on PDMS and goethite nanorods are for the first time approached from the perspective of the dielectric elastomers.

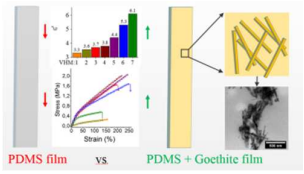

RSC Advances Accepted Manuscript

Journal Name

RSCPublishing

ARTICLE

Goethite Nanorods as Cheap and Effective Filler for Siloxane Nanocomposite Elastomers

-Cite this: DOI: 10.1039/x0xx00000x

M. Iacob[a,b], G. Stiubianu[a], C. Tugui [a], L. Ursu[a], M. Ignat[a], C. Turta[a,b] and M. Cazacu[a]

Received 00th January 2012,
Accepted 00th January 2012

DOI: 10.1039/x0xx00000x

www.rsc.org/

Iron oxide (goethite) with nanorod morphology was prepared by chemical precipitation method and characterized by FTIR, EDX, TEM, WAXD. This was used as an actve filler to prepare dielectric elastomer nanocomposites by its incorporation, besides silica, in a silicone matrix consisting in a high molecular weight polydimethylsiloxane-α,ω-diol (PDMS). The nanocomposites were processed as films, stabilized by peroxidic crosslinking at high temperature, and their properties of interest for potential use in the structure of electromechanical devices were studied. It is for the first time when such composites, based on PDMS and iron oxide in its well-defined type (goethite) and shape (nanorods) are approached from the perspective of the dielectric elastomers. The introduction of iron oxide nanoparticles in the polymer matrix resulted in improvements of both mechanical and dielectric properties. Thus the breaking strain and the dielectric constant values increased in comparison with those of the pure polymer sample, while the dielectric loss preserved low values specific for dielectrics.

Introduction

Polyorganosiloxanes exhibit exceptional properties as a result of Si-O-Si constituent unit in the polymer chain[1]: high flexibility of the polymeric chain, stability towards atomic oxygen, permeability for different gases, hydrophobic and anti-adhesive behaviour, physiological and chemical inertness, etc. This combination of properties leads to siloxanes being now found in almost all types of activities, from aviation and aerospace to household objects and devices, clothing and footwear, cosmetics, medicine and prosthetics, optics, electronics, etc. [2,3] In the last two decades is manifested great interest for silicones as dielectric elastomers.[4,5]

Elastomers built with polydimethylsiloxanes allow flexible membranes with low value of Young modulus, with application in electric actuator devices, taking advantage of forces and displacements larger than those in electrostatic or piezoelectric actuators. Researchers tested silicone rubbers as dielectric elastomer in actuators[6] due to inherent properties of siloxanes that make them useable in building actuation devices: large displacement with high precision and speed, high breakdown strength, reliability and low stiffness[7]. Silicones have elastic character but possess low values of dielectric constant, a factor which leads to large values of driving voltages that must be applied to silicone membranes in order to induce mechanical work[8].

Several types of inorganic fillers are incorporated within silicone to improve their dielectric permittivity: titanium dioxide, barium titanate, magnesium niobate, lead magnesium niobate–lead titanate, and strontium titanate.[2,3] Iron oxide, Fe_2O_3, is a traditional additive for silicone rubber that can impart increased thermal stability[2,3] but never has been studied its effect on the electromechanical behaviour of the silicone elastomers. In this paper, we are investigating the effect of the iron oxide, namely a well-defined form, goethite, on the properties of interest for the dielectric elastomers, mainly dielectric and mechanical. Thus, derivatives of the silicon and iron as the first (28%) and third (5%), respectively, most abundant metal in the Earth's crust are associated within a cheaper advanced material with potential application as a smart one (actuation and energy harvesting). This is a different approach from that recently published in which spherical iron oxide NPs were prepared and incorporated within a matrix consisting in a commercial silicone kit.[9] We used a polydimethylsiloxane-α-ω-diol (PDMS) of high molecular mass as matrix in which the goethite form of iron oxide as well-defined nanorods (size <100 nm) was incorporated by mechanical mixing as a disperse phase. The crosslinking of the composites was performed using high temperature peroxide radical initiator, which leads to chemically homogeneous samples. The association of these materials should lead to elastomer nanocomposites with good mechanical and dielectric properties. In addition, the well-known physiological inertness of siloxane[1] and the use of iron oxide nanoparticles in medical applications[10] create the premise to obtain new materials suitable for use by humans and not to affect in negative manner the environment.

Results and discussion

Nanoparticles preparation and characterisation

There are various methods for preparation of iron oxides nanoparticles with different shape and size, such as sol-gel[11], thermal decomposition[12], hydrothermal[13] or precipitation in basic medium[14]. For preparation of iron oxide nanoparticles we chose an affordable one step chemical precipitation method using iron chloride as the source for iron (Scheme 1). The precipitate containing the nanoparticles was purified by repeated washing until neutral pH and centrifugation. The nanoparticles were characterized using IR and Raman spectroscopy, transmission electron microscopy and wide angle X-Ray diffraction.

RSC Advances Accepted Manuscript

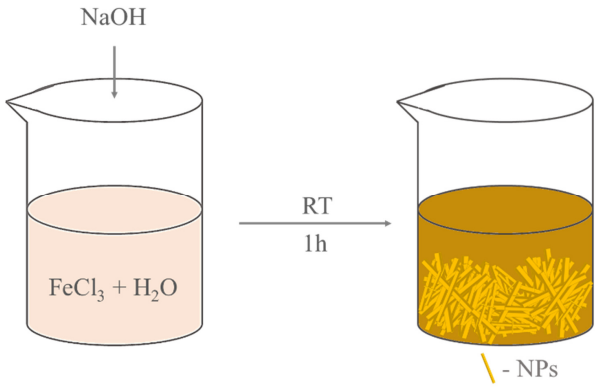

Scheme 1. Preparation of iron oxide nanoparticles.

The absorption bands present in the IR spectrum of goethite nanoparticles (Figure 1a) are attributable to OH and Fe-O vibrations. It was theoretically determined that there are 36 possible Fe-O vibrations and 12 hydroxyl vibrations, but not all of these were observed experimentally.[15] The band at 3107 cm^{-1} is assigned to stretching of OH groups located inside the nanoparticles and the one at 3478 cm^{-1} is assigned to the surface hydroxyl groups. OH bending bands are found at 893 cm^{-1} (δ_{OH} in plane bend) and 797 cm^{-1} (γ_{OH} out of plane bend). At 633 cm^{-1} and 399 cm^{-1} there are the bands assigned to symmetric and antisymmetric Fe-O vibrations. The position of all these bands are characteristic for α-FeOOH (goethite).[15] The presence of Fe in NPs was confirmed by EDX analysis (Figure 1b).

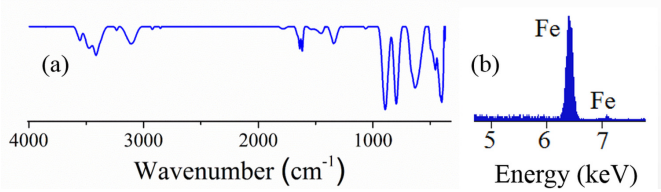

Figure 1. FTIR (a) and EDX (b) spectra for NPs sample.

The morphology of NPs was analysed by transmission electron microscopy (TEM), the images being presented in Figure 2. It can be seen that the NPs consist of nanorods with average size of 300 nm long and 35 nm diameter (Figure S1). As shown in Figure 2b, in the sample there is also irregular shaped material that might be the seeds from which nanorods grow.[16]

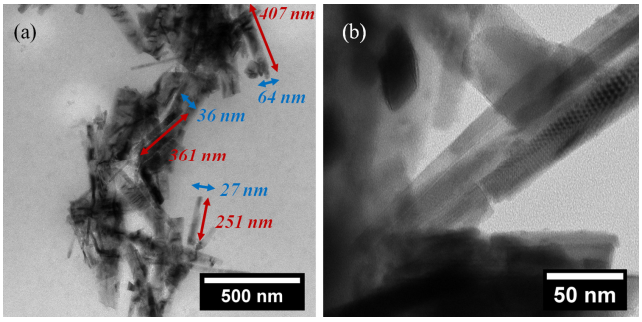

Figure 2. TEM images of NPs.

Wide angle X-Ray diffraction (WAXD) was used to identify the type of iron oxide (Figure 3a). The diffraction peaks revealed in the diffractogram of NPs coincide with those in the database characteristic for goethite (ICDD 29-0713). The Raman spectroscopy has been used as a complementary technique to FTIR and XRD in order to confirm the type of obtained iron oxide nanoparticles. The peaks present in the Raman spectrum of NPs (Figure 3b) at 206, 248, 301, 388, 482 and 549 cm^{-1}, are also characteristic for goethite phase.[15] Thus the results obtained by the three techniques, XRD, FTIR and Raman spectroscopies correlate well and confirm unambiguously the identity of goethite in the sample.

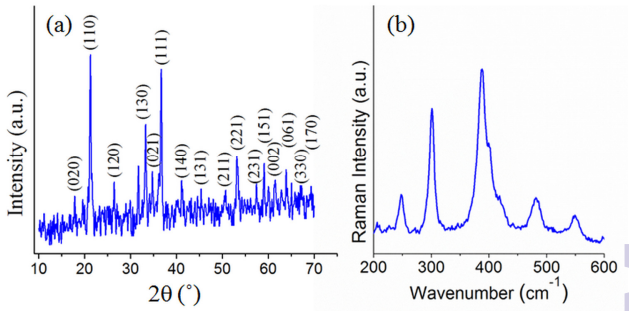

Figure 3. WAXD diffractogram (a) and Raman spectrum (b) of NPs.

Nanocomposites preparation and characterisation

The iron oxide nanorods obtained as described above were used as filler for silicone elastomer. The filler nanoparticles having high aspect ratio are desired since these leads to increased contact area with the polymer matrix, the filler being thus more effective in comparison with using spherical or cube nanoparticles. Silica as nanoparticles was used as co-filler being well-known for its mechanical reinforcing effect on the silicone rubber. A PDMS of high molecular mass (M_n=355500) was used as matrix. This is in fact a copolymer with a very low content of methylvinylsiloxane groups (around 0.04 mol%). The vinyl groups were inserted with the aim to facilitate the further peroxidic crosslinking. In order to have a clear image on the effect of each of the two fillers, multiple samples were prepared (Table 1): the reference sample VHM1 made only of pure siloxane without any nanoparticles, VHM2 with only 2 wt% goethite NPs, VHM3 with 20 wt% silica SD, and samples VHM4-VHM7 with both NP and SD in the composition, with increasing content of NP from 5 wt% (VHM4) up to 20 wt% (VHM7).

Table 1. The composition of the elastomer nanocomposites

Sample	NPs, g (wt%*)	SD, g (wt%*)
VHM1	0	0
VHM2	0.6 (2)	0
VHM3	0	3 (20)
VHM4	1.5 (5)	3 (20)
VHM5	3 (10)	3 (20)
VHM6	4.5 (15)	3 (20)
VHM7	6 (20)	3 (20)

* weight percentage in relation to PDMS matrix

Nanocomposite elastomers were prepared in a three-step procedure (Scheme 2): the first step consists in mixing and homogenizing the reagents on a double roll mixer, followed by a second step consisting in crosslinking the elastomer nanocomposite in an oven at 160-180 ºC under pressure. In this step, the benzoyl peroxide incorporated within composite decomposes homolitic to form two highly active radicals that rip hydrogen atoms randomly from the organic

RSC Advances Accepted Manuscript

This journal is © The Royal Society of Chemistry 20 2

(preferably vinyl) groups attached to the silicon atoms along the siloxane chains. The formed radicals quickly combine with each other leading to stable crosslinks (Scheme S1).[17,18] The third step consists in the aging of the elastomer at 180 ºC when the residual peroxides and decomposition products in the elastomer film were removed. The crosslinking data determined by extraction of the samples in toluene for 48 h under stirring at room temperature (Table S1) reveal high crosslinking yields, Cy (determined as a ratio between the dried sample masses after and before extraction), of about 0.970. The samples incorporating all components, inclusively the peroxide, but not submitted to the thermal crosslinking process were also behaved as crosslinked ones (Cy 0.923 and 0.945) showing very small percentages of soluble fraction, only slightly higher (0.055, 0.077) than chemically crosslinked samples (0.026-0.034). This is due to physical crosslinks (hydrogen bonds, hydrophobic interactions, etc.) known to be established between the components of the mixture during compound storage (about one year in this case). Regarding the integration of goethite nanoparticles into the composites, it is presumed that the OH groups on the surface of goethite nanoparticles will interact with benzoyl peroxide or its decomposition products[19] (Scheme S1) or even with Si-OH groups on the end of the PDMS chains. The consumption of the OH groups is proved by FTIR spectra of the crosslinked composites when are compared with that for single goethite (Figure S1). Thus, the band at 3478 cm^{-1} assigned to the hydroxyl groups on the surface of goethite NPs, and well visible also in the IR spectra of non-crosslinked composites, is completely absent in the spectra of the crosslinked ones, while those at 3107 and 800 and 900 cm^{-1} due to OH group inside NPs are still present in high intensities (i.e., VH7 composites. Figure S2).

The morphology and composition of the elastomer nanocomposites were studied by SEM/EDX, the dielectric characteristics were evaluated by dielectric spectroscopy and the mechanical properties were determined using stress-strain testing.

In Figure 4a-f are presented the SEM images of the cryofractured section of the film nanocomposites. Siloxane polymer chains tend to migrate at the surface of a composite material and therefore it is necessary to freeze the sample to be studied in liquid nitrogen and immediately fracture it. In comparison with sample VHM1 (Figure S3) made from pure siloxane with no filler added, the other samples present iron oxide nanoparticles and micrometer sized agglomerates. When silica nanoparticles are added in the composition (Figure 4b-f), the fracture has a more regular and clear breaking surface, with white silica nanoparticles agglommerates distributed in the polymer matrix. The distribution of the filler nanoparticles within t polymeric matrix (Figure 4g and 4h) is uniform with very few nanoparticles clumped together.

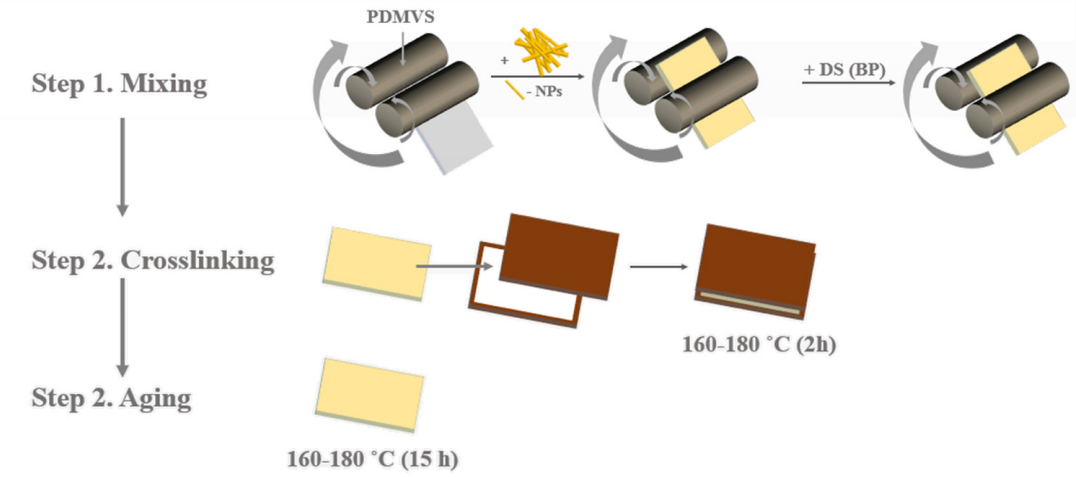

Scheme 2. Illustration of preparation procedure of elastomer nanocomposite films.

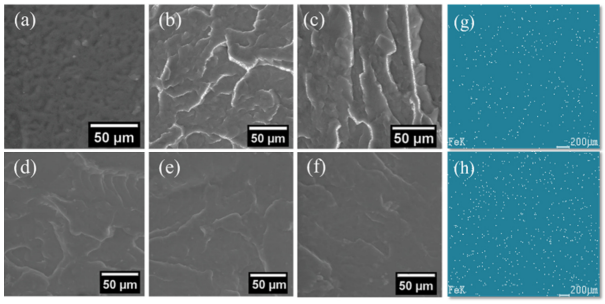

Figure 4. SEM images of nanocomposites: (a) VHM2, (b) VHM3, (c) VHM4, (d) VHM5, (e) VHM6, (f) VHM7, and EDX images for iron distribution in the samples: g) VHM2, h) VHM7.

The presence of iron oxide in the nanocomposite elastomers was also evidenced by XRF spectroscopy emphasizing iron atoms within matrix. The ratio of counts for iron and silicon suggest an increase in the content of iron oxide in the samples as visible in Figure 5, matching the experimental values of iron oxide added in preparation of the nanocomposites.

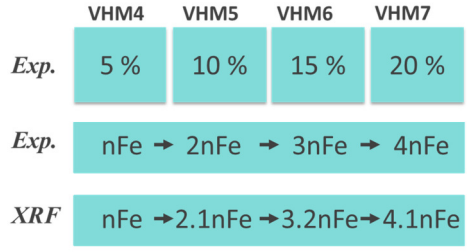

Figure 5. Correlation of XRF data (XRF) with experimental (Exp) values of iron oxide content in the samples.

The Raman spectrum registered on the nanocomposite VHM 7 (Figure S4) reveals the preservation of the goethite form by the presence of the characteristic bands at 246, 299, 384 and 486 cm^{-1}. In fact, according to literature,[15] the conversion of the goethite into

RSC Advances Accepted Manuscript

another form of iron oxide occurs in much harsher conditions (260 – 320 °C) than those to which the composite material was subjected during crosslinking.

The thermal behaviour of the crosslinked composite samples revealed by DSC is one characteristic for silicones not being affected in a fundamental way due to iron oxide presence. Thus, the DSC curves (Figure 6) show weak glass transition (T_g) in the range -120 ... -123 ºC, the limits corresponding to the pure siloxane polymer VHM1 (-120 ºC) and composite containing the highest content of goethite VHM7 (-123 ºC), respectively. The decrease in Tg value by raising filler content could happen as the nanoparticles well dispersed in the siloxane matrix increase the space between the chains allowing their easy sliding against each other, the more so as NPs are embedded in larger quantities. DSC data shows also the presence of an exothermic peak at about -71/-77 °C and an endothermic peak at -37/-41 °C) (Figure 6). These are attributed to the cold crystallization (~-75 °C) and melting of crystalline phase (~-40 °C). When the content of iron oxide nanoparticles increases (from 2% in VHM2 up to 20% in VHM7), the temperatures for the peak assigned to cold crystallization increase from around -76 up to -71 ºC and the area for the peak under the curve slightly decreases (Figure 6). Such behaviour suggests improved crosslinking and lower degree of freedom of the siloxane chains when there is a larger content of iron oxide nanoparticles, leading to formation of a small amount of crystalline phase at cooling (Figure 6).

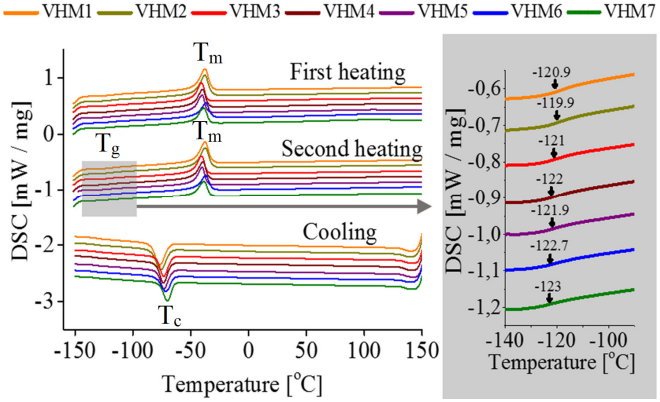

Figure 6. DSC measurements for the samples VHM1-7.

VHM1 sample containing siloxane polymer only has the lowest dielectric permittivity value on the entire studied frequencies range (10^0-10^6 Hz). The introduction of iron oxide nanoparticles (VHM2) or silica (VHM3) leads to a slight increase in the value of the dielectric constant of the film (Figure 7a). For samples VHM4-VHM7, with increasing concentration of NPs there is an increase in the value of the dielectric constant, the best results being for VHM7 sample, for which the dielectric permittivity values at 1 and 1000 Hz are 6.1 and 5.3, respectively (Figure 7a, Table 2). With the increase of the dielectric permittivity value an increase of the loss factor also occurs (Figure 7b). Increasing concentration of NPs in the films VHM4 - VHM7 has as result increased conductivity values (Figure 7d) from $3x10^{-14}$ (VHM4) up to 10^{-13} S/cm (VHM7) at 1Hz and from $8x10^{-12}$ (VHM4) up to $8x10^{-10}$ S/cm (VHM7) at 1000 Hz, but these are still specific values for electric insulator materials. With increasing frequency to 10^6 Hz, there is an increase of the conductivity value up to $5x10^{-8}$ S/cm. While both types of fillers used (silica and goethite) lead to improvement of the dielectric properties, it is clear from the charts that goethite nanorods have the largest effect at average content: 10 wt% (VHM5) and 15 wt% (VHM6).

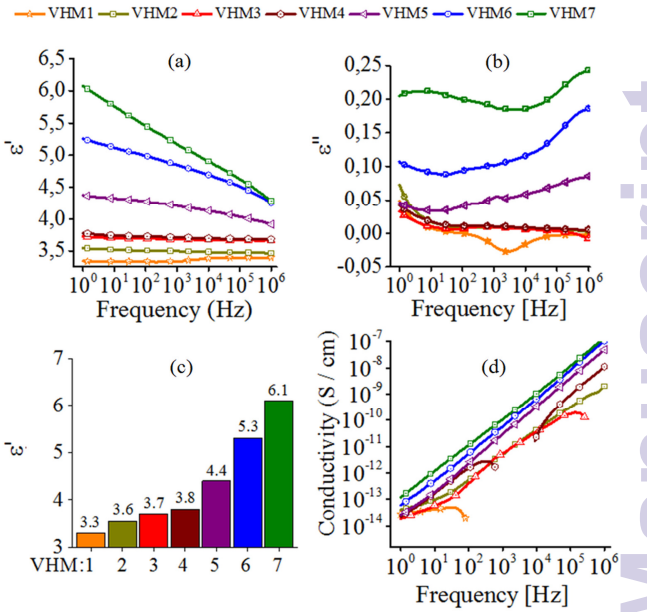

Figure 7. Dielectric tests for the elastomer nanocomposites: (a) dielectric constant as function of frequency, (b) dielectric loss as function of frequency, (c) the value of dielectric constant at 1 Hz and (d) conductivity values of elastomer nanocomposites as a function of frequency.

The film samples prepared as films with thickness of 0.5 mm were tested for electric breakdown strength, none of them suffering a breakdown at an applied voltage of 20 kV. Taking into account the fact that the film thickness was 0.5 mm can be estimated that the samples are resistant to a direct current of 40 MV/m.

In Figure 8 is presented the variation of the tensile load depending on tensile elongation for samples VHM1...VHM7. Samples containing no silica show lower tensile strength, manifested by lower values of load (MPa) and elongation (%) as percentage of initial length of the sample (VHM1, VHM2) (Figure 8, Table 2). Samples with silica nanoparticles in the composition show a clear improvement of the mechanical properties and adding small percentage (10%) of NPs leads to maximizing the mechanical strength of the elastomer sample (VHM5). Further increasing the percentage of NPs leads to gradually lower mechanical strength expressed as breaking stress (VHM5 > VHM6 > VHM7), and this is because when a larger percentage of nanoparticles are used in the composition, some of these aggregate and act as stress concentrators leading to earlier breaking under tensile stress.

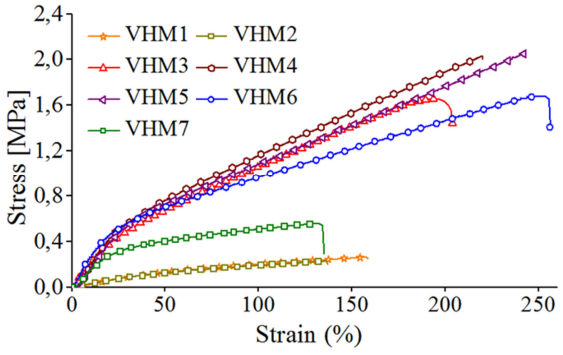

Figure 8. Stress-strain curves for samples VHM 1–7.

RSC Advances Accepted Manuscript

This journal is © The Royal Society of Chemistry 20 2

The results of stress-strain testing of the samples were used for the calculation of Young modulus. The value of Young's modulus (Y) impacts the behaviour of dielectric elastomers in both actuation and energy harvesting. When using dielectric elastomer membranes for actuation, the obtained strain is a result of the mechanical and electric properties of the dielectric elastomers[20], according to the following equation: $s = p/Y = (\varepsilon'\varepsilon_0 /Y) \cdot E^2$(1), where Y – the compression modulus in the thickness direction, ε' – the dielectric constant, ε_0 – the permittivity of free space, E – the electric field. Unfortunately, as can be seen, the increasing in mechanical resistance while the elongation increase is insignificantly leads to higher values for Young modulus.

The sorption of water vapours is an important characteristic when such dielectric elastomers are used in wet environments. In Figure 9 are presented the sorption/desorption isotherms at room temperature (25 ºC), with the total water uptake as percentage of dry sample mass as function of the environmental relative humidity for the samples VHM1-4 and VHM7. The shape of the sorption (s) and desorption (d) isotherms is similar for the tested samples. There is a clear, visible increase of the water vapour uptake in the samples as the relative humidity increases. Also the increase of the mass content of goethite nanoparticles leads to an increased water uptake, since the nanoparticles have large specific area and are not surface treated. In the hysteresis loop, the starting and the ending points do not superimpose and this is due to capillary condensed water present in the samples both before drying them for test and at the end of the desorption time. The shapes of the moisture sorption isotherms a type V, characteristic for hydrophobic materials with low porosity and with weak sorbent-water interactions[21].

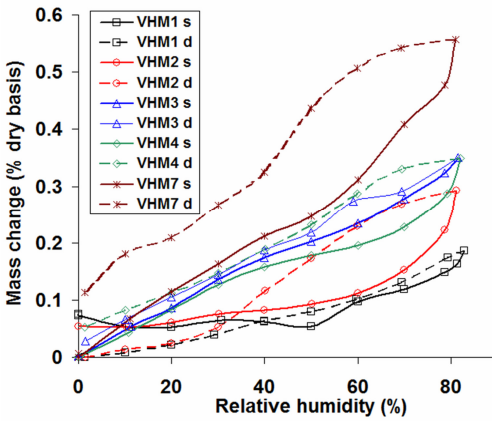

Figure 9. DVS measurements for prepared samples.

Table 2. Mechanical and dielectric properties related to actuation and energy harvesting

Sample	Breaking stress (MPa)	Stress at 10% elongation	Elongation at break (% initial length)	Young's modulus at 10% elongation[a] (MPa)	ε' (10 Hz)	ε'' (10 Hz)
VHM1	0.25	0.028	160	0.28	3.30	0.05
VHM2	0.20	0.034	140	0.34	3.55	0.07
VHM3	1.60	0.210	200	2.10	3.70	0.04
VHM4	2.00	0.190	220	1.90	3.75	0.04
VHM5	2.10	0.168	240	1.68	4.40	0.05
VHM6	1.55	0.208	250	2.08	5.25	0.11
VHM7	0.50	0.153	135	1.53	6.10	0.20

[a]A 10 % elongation is in the range of perfectly elastic deformation of the dielectric elastomer membranes, therefore the value of Young modulus was calculated at this value of elongation;

Experimental

Materials

Ferric chloride hexahydrate ($FeCl_3 \cdot 6H_2O$), supplied by Sigma Aldrich, purity 97%, was used as received. Polydimethylsiloxane-α,ω-diol (PDMS) of molecular mass Mn = 355500 and polydispersity index 1.5 (as estimated by GPC) was prepared in house, by already published procedure[17] consisting in equilibrium ring-opening polymerization of octamethylcyclotetrasiloxane in presence of 1 wt% concentrated sulphuric acid (96 %), at room temperature. A very small amount (0.6 mol%) 2,4,6,8-tetramethyl-2,4,6,8-tetravinylcyclotetrasiloxane was added in the reaction mixture in order to incorporate rare vinylsiloxane units along the siloxane backbone which only to facilitate the radical crosslinking. The procedure occurred in the following sequence: mixing 1 h, adding around 1 wt% water, mixing 0.5 h and left in the autoclave for almost 16 hours, polymer neutralization by repeated washings with sodium bicarbonate and cold water, drying at 110 ° C for 70 hours. Sodium hydroxide, NaOH (Fluka), with m.p. 318 ºC, d_4^{20}=2.13, purity >98 %, was used after grinding the pellets into fine powder in a mortar and drying in vacuum chamber. Benzoyl peroxide (BP), 40 wt% blend in dibutyl phtalate (Luperox AFR40) was supplied by Sigma-Aldrich. Fumed silica, Aerosil 2 (Degussa), (SD) 100% purity, specific surface 380 m^2/g, particle diameter 0.003-0.015 µm, was used after surface treatment. This consisted in drying in a vacuum oven, followed by hydrophobization using a treatment with 20% wt D_4 for up to 12 h at 160 ºC in a flask with condenser and with magnetic stirring of the silica.

Equipments

Gel permeation chromatography (GPC) in $CHCl_3$ was used for the determination of the molar mass of PDMS, using PL-EMD 950 Chromatograph-Evaporative Mass Detector that was calibrated with polystyrene standards before performing the measurements. Fourier transform infrared (FTIR) spectra were recorded with a Bruker Vertex 70 FTIR spectrometer, in transmission mode in the range 400-4000 cm^{-1}, at room temperature with KBr pellets, with collection of 32 scans and a resolution of 2 cm^{-1}. of Energy-Dispersive X-ray Fluorescence (EDXRF) measurements were performed with EX-2600 X-Calibur SDD (30 µA, 15 kV, 200 s range 10 keV in vacuum) in order to determine the elemen composition of samples. As results of the measurements were identified the Kα1 peak for elements and its intensity (in Counts) and the samples were measured at least twice on each side. A dedicat d HITACHI HT7700 microscope was used to perform t Transmission Electron Microscopy (TEM) in high contrast mode u

RSC Advances Accepted Manuscript

to 100 kV accelerating voltage. For this purpose small droplets of the diluted dispersion (~1g/L) of iron oxide nanoparticles were placed on 300 mesh carbon coated copper grids and dried in vacuum at 50 ºC. Powder X-ray diffraction analysis (PXRD) was used as method to identify the phases in powder and for this was used an instrument BRUKER D8 ADVANCE diffractometer (XRD) with anode of Cu with kα1 = 1.5406 and the following conditions: the range for recording the spectra was 2θ = 20÷100° and 2θ = 20÷80° with a time/step of 0.5 sec/step and 1 sec/step, the size of the scan step was 0.01 and 0.02 respectively, the tension applied to the tube was 40 kV, the intensity of the current was 30 mA and the working temperature of 25 °C. The Renishaw InVia Reflex spectrometer with a 632.8 nm HeNe laser as excitation source was used for the determination of the Raman spectra in the spectral region 100-1000 cm^{-1}. The laser beam was focused on the sample and the backscattered Raman signal with a 50x objective lens with NA= 0.75 of a Leica DM 2500M microscope. The samples were investigated at low incident laser power in order to avoid sample degradation. Dielectric spectra were recorded with Novocontrol "Concept 40" broadband dielectric spectrometer (Hundsangen, Germany). The samples had uniform thickness (1 mm) and were mounted between gold platens. The experiment was carried out at fixed room temperature (25 ºC) and sweeping the frequency: 1–100000 Hz. The dielectric constant (ε') and loss (ε") were recorded. Stress–strain measurements were performed using TIRA test 2161 apparatus, Maschinenbau GmbH Ravenstein, Germany at room temperature. For this purpose, the samples were cut in dumbbell shapes (50x8.5x4 mm). The samples were strained with a rate of 20 mm/min. Each sample was measured three times and the average value was taken into consideration. The error bars are not shown in the stress-strain chart since the error deviations were less than 5% of the average. The measurements for electric breakdown strength were performed on a Trek installation consisting of: high-speed high-voltage power amplifier, function generator, and oscilloscope. The electrodes consisting of iron discs with 2.5 cm diameter were applied on the film samples and the measurements were performed with a voltage increase rate of 2000 $V \cdot s^{-1}$ at room temperature (20 ºC). Before the measurements, all the samples were maintained in the equipment room in order to reach equilibrium with the environmental humidity.

Preparation of iron oxide nanoparticles (NPs)

The starting point for the preparation of iron oxide nanoparticles is the classic method of precipitation[14] but we chose the ratio of reagents in order to achieve nanorods, as was established by preliminary tests. 100 g of $FeCl_3$ were dissolved in 700 ml double distilled water. 50 g of NaOH were added in the mixture and allowed to stir with a magnetic stirrer for up to 1 h. The resulting precipitate was repeatedly washed with distilled water and centrifuged until a neutral pH was achieved. IR (KBr): ν (cm^{-1}) = 399vs, 455m, 633s, 797vs, 893vs, 1639w, 3101w, 3235vw, 3414m, 3478w, 3553w.

Preparation of nanocomposite elastomers

30 g of PDMS and pre-established amount of fillers (iron oxide and/or silica nanoparticles), according to Table 1, were thoroughly mixed in a double roll mixer, followed by incorporation of 2 wt% BP (on the roll). The resulting mixture is put in a mold with a frame with sides of 100x100 mm and a height of 1 mm, and then pressed between two plates and held in an oven at 160-180 °C for 1.5 - 2 hours. Then the film was released from the mold and kept for 15h at 180 in air flow oven to remove residual decomposition products of the peroxide and aging.

Conclusions

The as prepared goethite nanoparticles and polydimethylsiloxane-α,ω-diol synthesized in house were used for the first time in the preparation of dielectric elastomer nanocomposites as films, through a simple affordable procedure. XRF analysis results of the crosslinked composite films reveals a rather uniform distribution of the iron within material bulk, while Raman spectroscopy proves the preservation of the goethite form of the iron oxide, not altered during the process of peroxidic curring at elevated temperature. The DSC data revealed that the thermal behaviour of elastomer nanocomposites is not significantly different than that of pure siloxane, proving the nanoparticles of iron oxide and silica used as fillers were well incorporated in the siloxane polymer matrix. Although one would expect the large percentage of nanoparticles used in the composition to make these materials conductive, the films were homogeneous and had good dielectric behaviour: low conductivity values ($\sigma < 10^{-7}$ S/cm), dielectric constant values (3.5 – 6.1) larger than that of pure siloxane films (ε' = 3.1), while the loss factor is maintained at low values (ε" < 0.2) and EBD value above 40 V/μm. The use of goethite nanorods also improves the mechanical properties of the samples in comparison with those of pure siloxane (VHM1). Unfortunately, Young modulus also increases by filler incorporation that could affect the using of the elastomeric films in actuators or energy harvesting devices but there are perspectives for another applications, e.g., in sensors.

Acknowledgements

This work was supported by a grant of the Ministry of National Education, CNCS – UEFISCDI, project number PN-II-ID-PCE-2012-4-0261 (Contract 53/02.09.2013), national project number No. 14.518.02.05A and project PolyWEC (www.polywec.org, prj. ref 309139), a FET-Energy project that is partially funded by the 7th Framework Programme of European Community and co-financed by UEFISCDI (Contract 205EU).

Notes and references

[a]"Petru Poni" Institute of Macromolecular Chemistry, Iasi, 700487, Romania; mcazacu@icmpp.ro.
[b]Institute of Chemistry of ASM, Academiei str. 3, Chisinau 2028, Republic of Moldova; turtalcba@gmail.com.

†Electronic Supplementary Information (ESI) available: SEM image of VHM1, Raman spectrum of VHM7. See DOI: 10.1039/b000000x/

1 W. Noll, *Chemistry and technology of silicones*, Academic Press, New York, 1968.
2 N. B. Madsen, Risø National Laboratory, Roskilde, Denmark, 1999.
3 M. Bengtsson, K. Oksman and N. M. Stark, *Polym. Compos.*, 2006, **27**, 184–194.
4 A. Bele, M. Cazacu, G. Stiubianu and S. Vlad, *RSC Adv.*, 2014, **4**, 58522–58529.
5 F. B. Madsen, L. Yu, A. Daugaard, S. Hvilsted and A. L. Skov, *RSC Adv.*, 2015.
6 N. Gharavi, M. Razzaghi-Kashani and N. Golshan-Ebrahimi, *Smart Mater. Struct.*, 2010, **19**, 025002.
7 E. Tuncer and I. Sauers, in *Dielectric Polymer Nanocomposites*, ed. N. J. Keith, Springer, New York, 2009, p. 321.
8 Y. Bar-Cohen and Q. Zhang, *MRS Bull.*, 2011, **33**, 173–181.
9 F. Pisanello, R. De Paolis, D. Lorenzo, S. Nitti, G. Monti, D. Fragouli, A. Athanassiou, L. Manna, L. Tarricone, M. D

This journal is © The Royal Society of Chemistry 20 2

RSC Advances Accepted Manuscript

Vittorio and L. Martiradonna, *Microelectron. Eng.*, 2013, **111**, 46–51.
10 C. de Montferrand, L. Hu, I. Milosevic, V. Russier, D. Bonnin, L. Motte, A. Brioude and Y. Lalatonne, *Acta Biomater.*, 2013, **9**, 6150–7.
11 J. Xu, H. Yang, W. Fu, K. Du, Y. Sui, J. Chen, Y. Zeng, M. Li and G. Zou, *J. Magn. Magn. Mater.*, 2007, **309**, 307–311.
12 M. Iacob, M. Cazacu, C. Racles, M. Ignat, V. Cozan, L. Sacarescu, D. Timpu, M. Kajňaková, M. Botko, A. Feher and C. Turta, *RSC Adv.*, 2014, **4**, 6293.
13 J. Wang, J. Sun, Q. Sun and Q. Chen, *Mater. Res. Bull.*, 2003, **38**, 1113–1118.
14 S. Laurent, D. Forge, M. Port, A. Roch, C. Robic, L. Vander Elst and R. N. Muller, *Chem. Rev.*, 2008, **108**, 2064–110.
15 R. M. Cornell and U. Schwertmann, *The Iron Oxides: Structure, Properties, Reactions, Occurences and Uses, Second Edition*, Wiley-VCH, Weinheim, Wiley-VCH., 2004.
16 Z. Wei and F. P. Zamborini, *Langmuir*, 2004, **20**, 11301–4.
17 M. Cazacu, C. Racles, A. Vlad, M. Antohe and N. Forna, *J. Compos. Mater.*, 2009, **43**, 2045–2055.
18 S. C. Ganguly, in *Macromolecules Containing Metal and Metal-Like Elements, Group IVA Polymers*, eds. A. S. Abd-El-Aziz, C. E. Carraher, C. U. Pittman and M. Zeldin, John Wiley & Sons, Hoboken, 2005, pp. 161–202.
19 O. J. Walker and G. L. E. Wild, *J. Chem. Soc.*, 1937, 1132.
20 R. Pelrine, *Science (80-.).*, 2000, **287**, 836–839.
21 S. J. Gregg and K. S. W. Sing, *Adsorption, surface area, and porosity*, 1991.

RSC Advances Accepted Manuscript